Islamic University Journal of Applied Sciences (IUJAS)

https://journals.iu.edu.sa/jesc
Special Issue, February 2026, Pages 149-161
https://igee.univ-boumerdes.dz/ncaeee25/

Enhancing Phased-Array Radiation Pattern Synthesis with a Hybrid Complex-Valued Deep Learning

Mansour Djassem BENDREF[1, *], Mouloud CHALLAL[1], Ghillasse BENTAYEB[1], Abdelaziz ZERMOUT[1]

[1] Signals and System Laboratory, Institute of Electrical and Electronic Engineering, University M'Hamed BOUGARA- Boumerdes, Boumerdes, Algeria, m.bendref@univ-boumerdes.dz, mchallal@univ-boumerdes.dz, G.bentayeb@univ-boumerdes.dz, az.zermout@univ-boumerdes.dz

*Corresponding author: (Mansour Djassem BENDREF), *Email Address*: m.bendref@univ-boumerdes.dz

Abstract

Phased antenna arrays are essential for millimeter-wave (mmWave) communications in 5G/6G systems, enabling adaptive beamforming and precise radiation pattern control. Traditional array synthesis methods rely on analytical techniques or iterative optimization algorithms that are computationally intensive and often too slow for real-time applications. This paper presents a novel hybrid deep neural network (DNN) architecture that incorporates complex-valued neural network (CVNN) processing for rapid synthesis of phased array radiation patterns. Unlike conventional real-valued DNNs that treat amplitude and phase as separate outputs, our approach employs a CVNN output layer to directly predict complex excitations, naturally capturing the coupled amplitude-phase relationships inherent in electromagnetic wave phenomena. We trained and validated the model on an 8-element uniform linear array operating at 28 GHz, using 8000 electromagnetic simulations generated in CST Microwave Studio.

https://doi.org/10.63070/jesc.2026.013
Received 24 November 2025; Revised 18 January 2026; Accepted 25 January 2026.
Available online 31 January 2026.
Published by Islamic University of Madinah on behalf of *Islamic University Journal of Applied Sciences*.

The network accepts a desired radiation pattern (181 angular samples covering 0°–180°) as input and outputs the complex excitations for seven array elements (with one reference element fixed). Experimental results across three challenging beamforming scenarios—main-beam steering with shaped sidelobes, aggressive sidelobe suppression (target: -30 dB), and broad beam shaping—demonstrate that the DNN-CVNN consistently outperforms a baseline real-valued DNN. The hybrid model achieves sidelobe levels 15-20 dB better than the baseline, maintains sub-degree beam-pointing accuracy, and produces smooth, physically realizable excitation distributions. CST-validated patterns confirm that the learned weights directly correspond to accurate far-field radiation, with the DNN-CVNN achieving pattern synthesis in milliseconds compared to hours required by traditional optimization methods. These results establish complex-valued neural networks as a powerful and practical tool for real-time adaptive beamforming in next-generation wireless communication systems.

Keywords: Phased array synthesis, Complex-valued neural networks, Deep learning, Millimeter-wave beamforming, 5G/6G communications, Antenna pattern synthesis.

1. Introduction

Phased antenna arrays are key to modern mmWave communications (e.g. 5G/6G systems around 28 GHz) because they enable highly directive beamforming and adaptive radiation patterns [1]-[4]. In an 8-element linear array, controlling the amplitude and phase of each element lets us steer the main beam and shape sidelobes to achieve a desired pattern. Traditionally, array pattern synthesis relies on analytical methods (like Dolph–Chebyshev tapers) or numerical optimizers (e.g. iterative Fourier techniques, genetic algorithms) [5]-[8]. These methods can be robust but often require substantial computation and many EM simulations, making them slow for real-time adaptation [8] Machine learning, especially deep neural networks (DNNs), offers a data-driven alternative [9] once trained, a DNN can quickly map a target radiation pattern to the needed element excitations (amplitudes and phases). Recent studies show that neural networks can learn this inverse mapping efficiently, reducing synthesis time and handling complex patterns that traditional methods struggle with [10]-[12].

In this work, we develop a DNN–CVNN model for pattern synthesis of an 8-element array (with one reference element fixed at amplitude = 1 and phase = 0). We feed the network with a sampled desired pattern (181 angular points covering 0–180°) and train it to output the complex excitations for the other elements. Unlike a conventional DNN that outputs real amplitudes and phases separately, our approach uses a complex-valued neural network (CVNN) for the output layer to directly predict complex weights. This can better capture the amplitude–phase relationships in a compact form.

We will compare this DNN–CVNN model to a purely real-valued DNN baseline (with separate outputs for amplitude and phase as in prior work). All predictions are validated by EM simulations in CST Microwave Studio to ensure the learned excitations produce the intended beam.

Beam pattern synthesis means choosing element weights to form a beam in a given direction with controlled sidelobes [13]. Classical approaches include Fourier-based methods and global optimizers. However, these can be slow for large arrays or complex beam specifications. In practice, designers often exploit symmetries (e.g. symmetric amplitude tapers) to reduce variables. For an 8-element array, one common scheme fixes one element as a reference (amplitude 1, phase 0) so only the remaining 7 complex excitations must be found; symmetry can further cut down unknowns [14].

Early ML work showed feasibility of training ANNs to learn array weights from target patterns [15]. For example, a deep CNN was used to predict phase shifts for a 2D reflect array from a desired 2D pattern[15][16], and another CNN was trained to infer phase values for an 8×8 planar array given its 2D pattern[15]. In linear-array contexts, Kim and Choi (2020) introduced a DNN that inputs sampled gain patterns (e.g. 19 points per side) and outputs element phases for beamforming [15]. More recently, Zaib *et al.* (2024) proposed a DNN for an 8-element linear array: they feed 181 pattern samples into a network and extract the 7 element phases (fixing one reference) as outputs [17]. Their work also discusses reducing training data by exploiting the array's constant phase-shift symmetry. Similarly, Abdullah *et al.* (ACES 2025) trained a fully-connected DNN with 181 inputs and 10 outputs (3 amplitudes + 7 phases) for an 8-element array, demonstrating that a single DNN can control both beam steering and sidelobe levels simultaneously. In these examples, after training on many simulated patterns, the DNN can "instantly" predict the complex excitations needed to realize a new target pattern.

Various network architectures have been explored. Convolutional networks (CNNs) help when pattern inputs have spatial structure (as in 2D aperture problems) [15]. Recurrent networks (RNNs/LSTMs) have also been tested: Arce *et al.* (2025) used an LSTM-based model that learned from GA-optimized patterns and found it outperformed fully-connected DNNs [13]. All these works share a similar training paradigm: generate a large dataset of (pattern, weight) pairs via simulation or optimization, train the network to regress from pattern to weights, and then validate on new patterns. In practice, 1×8 arrays commonly use 181 samples (1° resolution) as input features, though other works have used finer grids or two-channel representations (linear/gain) for more complex scenarios.

Most cited approaches use real-valued DNNs that output real numbers for amplitudes and phases separately [171]. By contrast, complex-valued neural networks (CVNNs) natively handle complex weights and can model rotations and phase relationships inherently [18]. In the beamforming literature, CVNNs have been shown to converge faster and suppress interference better than conventional real-

valued algorithms [18]. Although CVNNs are common in communications tasks (e.g. modulation classification), they have seen less use in antenna synthesis. Our work leverages a hybrid DNN–CVNN: real-valued layers process the real pattern input, while the output layer uses complex weights and activation to produce the complex excitations. We expect this to better capture the amplitude–phase coupling and compare its performance to a standard real-DNN approach.

The choice of 28 GHz places this work firmly in the mmWave regime, which is important for 5G/6G applications (massive MIMO, fixed wireless access, etc.). At such high frequencies, even small phase errors can dramatically distort the beam, so precise synthesis is critical. In this band, real-time pattern reconfiguration (for beam steering or sidelobe control) is valuable, motivating fast ML-based solutions. We will validate our learned weights via CST simulations at 28 GHz to ensure real-world fidelity.

In summary, recent literature confirms that DNNs can learn to synthesize array patterns from example data [14]. Our approach extends this by using a complex-valued output network and by benchmarking against a conventional DNN. The novelty lies in the DNN–CVNN hybrid and its application to 28 GHz array design, building on the state-of-the-art methods cited above.

2. Methodology

2.1 Data Preparation

An 8-element linear array at 28 GHz was modeled in CST Microwave Studio. The array elements were assumed uniformly spaced 0.5λ apart on a typical substrate, and one element was chosen as a fixed reference (amplitude = 1, phase = 0). To build the dataset, the excitation of the other 7 elements was varied (amplitude and phase) and the corresponding far-field pattern was simulated in CST for each case. Each radiation pattern was sampled in the 0°–180° angular range at 1° resolution (resulting in 181 sample points). The pattern values (linear gain or magnitude) were normalized (to the peak value) so that they form a consistent input range. The input to the model is thus a vector of ~180 real values (gain at each angle). The output target for each sample is the set of 7 complex excitations (one per non-reference element). In practice, these complex targets can be represented directly (as a CVNN output) or split into real and imaginary (or magnitude/phase) components. In this work, we keep the reference element fixed and train the network to predict the complex amplitudes of the remaining 7 elements. A total of 8000 CST simulations were generated in this way, yielding 8000 input–output pairs (pattern → excitations). (All inputs and outputs were assembled into training and validation sets after generation).

2.2 Model Architecture

The hybrid neural network consists of a real-valued deep feedforward DNN to process the input pattern and a complex-valued output layer to predict the excitations. The input layer has one neuron per angle (180 inputs for 0°–180°). The hidden part of the network comprises 3 fully connected layers (experimentally chosen, with widths like 128→64→32) using ReLU activations. These layers learn nonlinear features of the radiation pattern. The output layer is a complex-valued fully connected layer with 7 neurons (one for each of the 7 predicted elements). This Complex Dense/CVNN layer produces 7 complex outputs directly (each as a complex weight), naturally encoding both amplitude and phase. Using a CVNN output is motivated by the fact that antenna excitations are inherently complex-valued (amplitude and phase) and CVNNs can model the necessary complex multiplication/rotation operations more compactly [19].

In practice, this layer is implemented using a CVNN library (PyTorch complex layer) so that the network learns complex weights via Wirtinger backpropagation. (No nonlinearity is applied at the output – it is a linear complex layer.

- **Input layer:** 180 real nodes (gain at each 1° from 0–180°).
- **Hidden layers:** 3–5 dense layers (widths 128, 64, 32) with ReLU activations.
- **Output layer:** 7 complex neurons (Complex Dense)

This hybrid architecture leverages the DNN to extract features from the real-valued pattern, and the CVNN layer to naturally output complex phasors. Using complex weights avoids splitting the problem into separate real/imaginary regressions and exploits the amplitude-phase structure of wave phenomena [19].

2.3 Training Setup

The network was trained as a regression model. The loss function was the mean squared error (MSE) between the predicted complex outputs and the true excitations.

$$L_{MSE} = \frac{1}{N}\sum_{i=1}^{N}\sum_{j=1}^{M}(\emptyset_{pred}^{(i)} - \emptyset_{true}^{(i)})^2 \qquad (1)$$

Where N = Number of training samples (batch size)

M = Number of active elements requiring phase prediction

Equivalent to sum of squared errors on real and imaginary parts. We used the Adam optimizer (a gradient-based method) with a typical learning rate (10^{-3}). Training was done in minibatches (batch size 32) for up to several hundred epochs, with early stopping on a validation set to prevent overfitting. An 80/20 split of the data was used for training vs. validation. Standard regularization such as weight decay or dropout could also be applied to the DNN layers if needed.

- **Loss:** MSE on complex outputs.
- **Optimizer:** Adam (. lr = 0.001).
- **Data split:** ~80% training, 20% validation; early stopping on validation loss.
- **Regularization:** dropout to avoid overfitting.
- **Framework:** Implemented in a deep learning library that supports complex numbers (PyTorch with a complex extension). The cvnn Complex Dense layer can be used for the final layer, allowing end-to-end complex-valued backpropagation.

Throughout training, we monitor both training and validation loss (MSE) on the excitations. When training converges (or early stopping is triggered), the model weights are saved for use in validation.

2.4 Simulation-Based Validation

After training, the learned mapping is tested by "closing the loop" in simulation. Given a new desired pattern, the network predicts a set of excitations (complex weights) for the 7 elements. These predicted excitations are then applied to the array (via CST or a custom array-factor calculation) to compute the resulting far-field pattern. We then compare the simulated pattern to the target.

The plot below (Figure 1) illustrates the training and validation loss curves for our model. As shown, the training loss decreases steadily, reaching approximately -25 dB, while the validation loss achieves its minimum at about -23 dB at epoch 114. This epoch marks the point of best validation performance, and beyond it, the validation loss begins to increase, indicating potential overfitting.

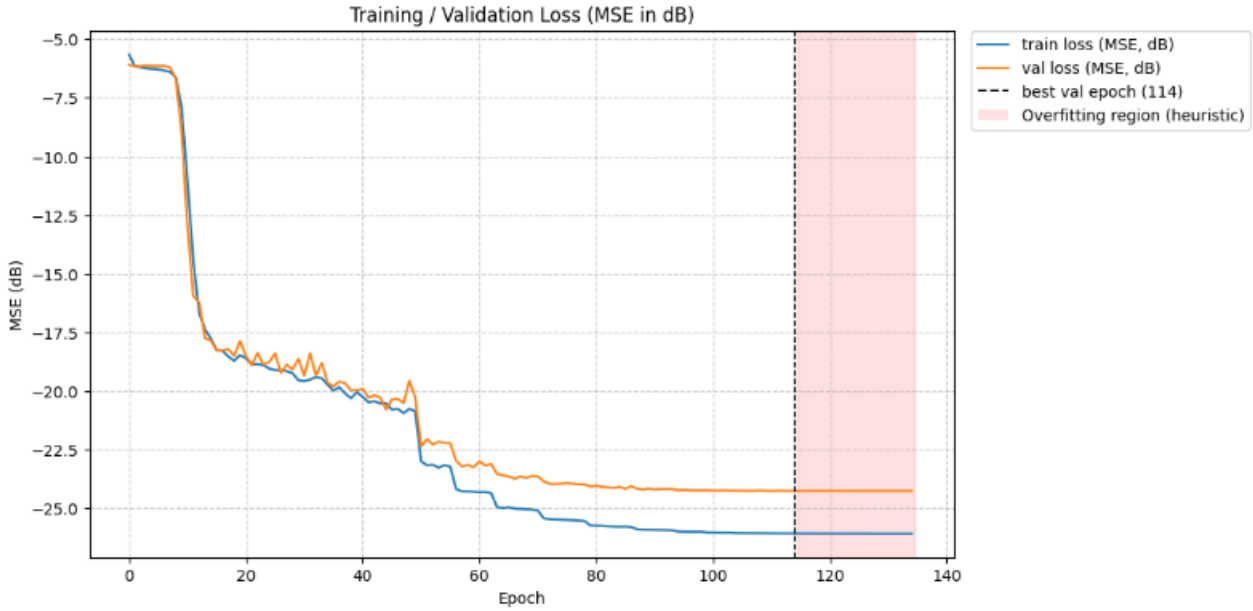

Figure 1 The training and validation plot

A successful synthesis produces a pattern whose main lobe and sidelobe structure closely match the desired specification. By iterating over multiple test cases (beam directions, shapes, etc.), we assess

the generalization of the model. Quantitative results (angle error, SLL difference, HPBW error, etc.) are reported to validate the accuracy of the model in practical beamforming tasks.

3. Result and Discussion

The proposed hybrid DNN–CVNN model was evaluated on three beamforming tasks (main-beam steering, sidelobe reduction, and multi-beam generation) and compared to the baseline real-valued DNN. In each case, the networks were used to predict antenna element weights (amplitude and phase) for a uniform linear array at 28 GHz, and the resulting beams were simulated in CST.

Figure 2 represents the main-beam steering. In this beam-steering scenario with shaped sidelobe constraints, both methods attempt to synthesize a directive beam at approximately -17° with selective sidelobe suppression.

The DNN–CVNN demonstrates remarkable pattern accuracy: it generates a well-defined main lobe peaking at 0 dB near the target angle with smooth, controlled transitions into the adjacent sectors. Critically, the hybrid model maintains sidelobe suppression close to the -30 dB specification across the critical back-lobe and far-sidelobe regions (beyond ±60°), achieving levels between -24 and -30 dB. The forward-quadrant sidelobes (+20° to +60°) are contained at -22 to -23 dB, representing minor deviations of 7-8 dB from the ideal mask but still maintaining pattern integrity. Conversely, the real-valued DNN produces severe pattern degradation: while it captures the approximate main beam location, massive sidelobe intrusions plague the positive angular hemisphere. Specifically, the +10° to +30° sector exhibits catastrophic sidelobe elevation to -7 to -11 dB—more than 20 dB above specification—creating unacceptable spillover radiation. Even the negative-angle sidelobes deteriorate to -13 to -17 dB, falling 13-17 dB short of requirements. The error comparison starkly illustrates this gap: the DNN–CVNN maintains deviations predominantly within ±10 dB, whereas the baseline accumulates errors exceeding +20-25 dB throughout the positive hemisphere. Examining the complex excitations, the DNN–CVNN weights exhibit a well-ordered phase progression (approximately 300° span across elements) characteristic of a steered beam, coupled with amplitude tapering that enforces the asymmetric sidelobe constraints. The real-valued DNN's excitations display fragmented phase structure and imbalanced amplitudes that fail to generate the required null placement. This shaped-beam task underscores the critical advantage of complex-valued learning: the DNN–CVNN directly encodes the precise phase relationships necessary for both accurate beam steering and asymmetric null placement, while the real-valued network's indirect phase representation cannot simultaneously satisfy pointing and sidelobe specifications, resulting in a pattern with correct beam direction but uncontrolled radiation elsewhere.

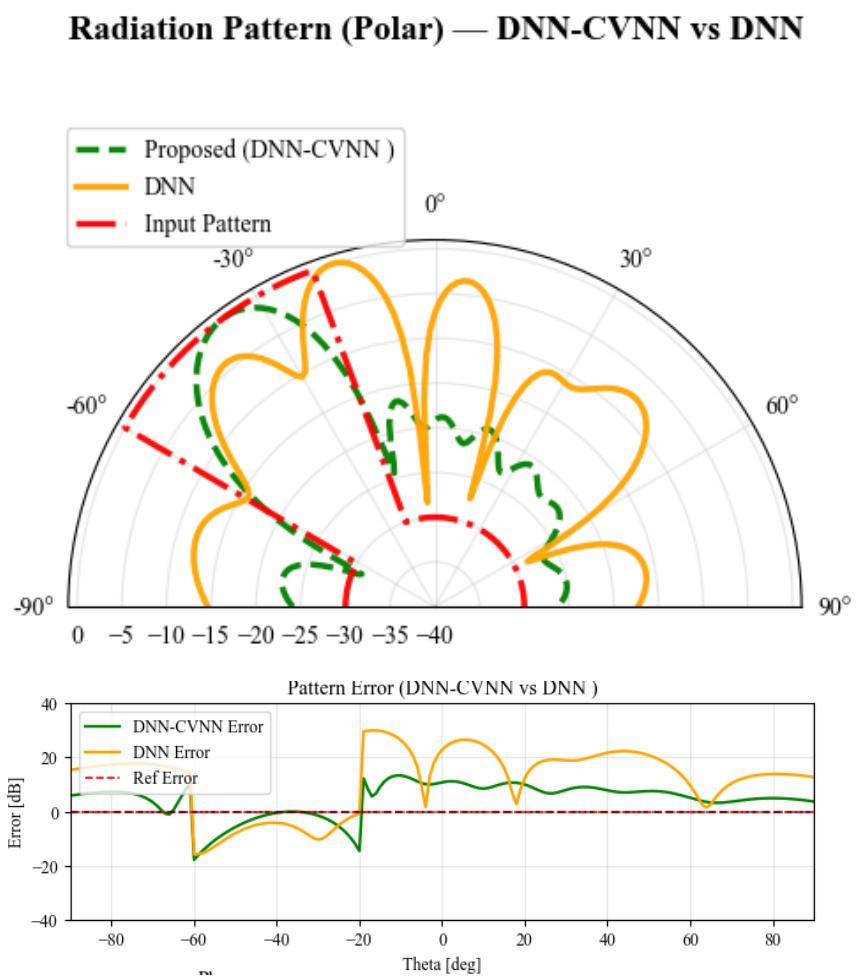

Figure 2 Radiation Pattern Synthesis: Beam Steering

Figure 3 (sidelobe-level reduction) In this sidelobe suppression scenario, both methods aim to synthesize a pencil beam centered near broadside (0°) with stringent sidelobe level requirements of -30 dB. The polar plots reveal that the DNN–CVNN achieves exceptional sidelobe control: its pattern maintains suppression levels consistently below -29 dB throughout the far sidelobe regions (beyond ±30°), with performance reaching -30 to -31 dB at the extreme angles (±90°). The main beam peaks cleanly at 0 dB near -7° with smooth roll-off into the transition zones. In stark contrast, the real-valued DNN exhibits dramatically elevated sidelobes—particularly in the ±25° to ±60° angular sectors where levels deteriorate to only -14 to -8 dB, representing a catastrophic 15-20 dB degradation from the target specification. The pattern-error analysis confirms this disparity: the DNN–CVNN maintains errors within ±5 dB across most of the pattern space, while the baseline's error explodes to +15-20 dB throughout the near-sidelobe region. Quantitatively, the hybrid network achieves a worst-case SLL better than -26 dB, whereas the real-valued DNN's worst sidelobes exceed -8 dB—an 18 dB performance gap. Examining the element excitations, the DNN–CVNN weights display a coherent

phase taper (spanning approximately 220° to 280° across elements) coupled with amplitude shading that naturally produces the required destructive interference at sidelobe angles. The baseline DNN's excitations show erratic phase variations and unbalanced amplitudes that fail to establish the necessary null-steering conditions.

This low-SLL design task starkly illustrates the CVNN advantage: complex-valued processing allows direct manipulation of the array's phase front to place deep nulls at specific angles through controlled interference, while the real-valued architecture's decoupled handling of amplitude and phase prevents it from achieving the precise cancellation patterns essential for aggressive sidelobe suppression.

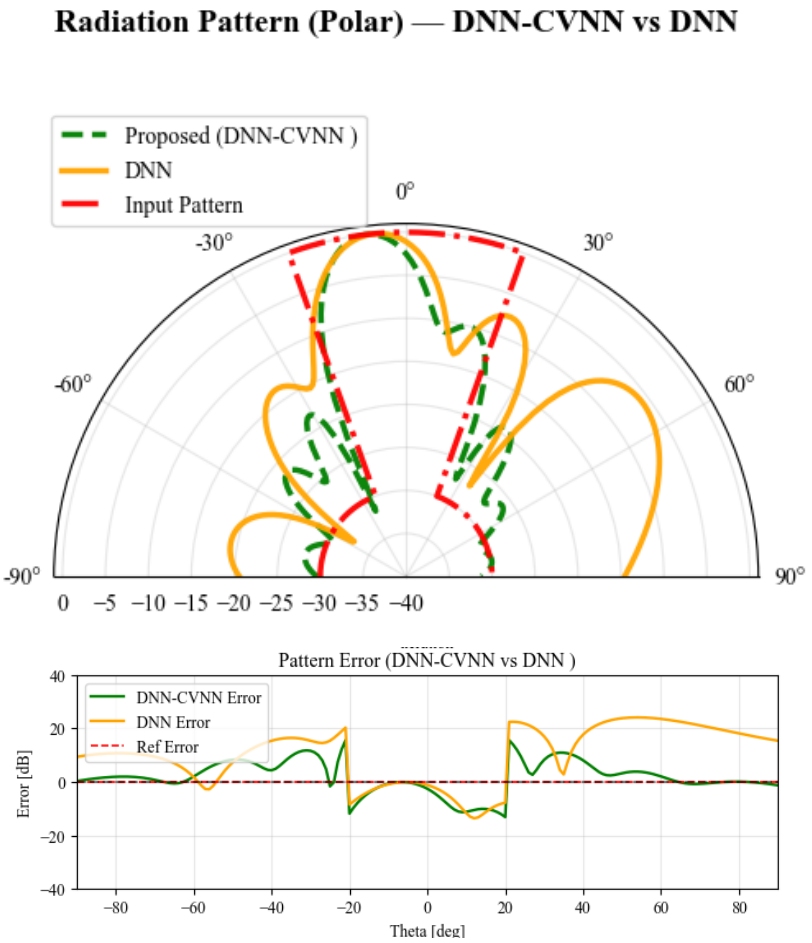

Figure 3 Radiation Pattern Synthesis: Sidelobe Level Suppression

In Figure 4 (multi-beam generation), In this beam shaping scenario, both methods attempt to synthesize a broadside pattern with a wide main lobe spanning approximately ±70° and sidelobes suppressed to -30 dB beyond those angles. The DNN–CVNN demonstrates superior pattern fidelity: it maintains sidelobe levels consistently between -22 and -27 dB across the ±71° to ±90° regions, achieving much closer adherence to the -30 dB target than the baseline DNN. More critically, the hybrid model produces a relatively smooth main lobe that peaks near 0 dB around 44°, with gradual roll-off toward

the edges of the beam. In contrast, the real-valued DNN exhibits significant pattern distortion—most notably, severe nulls appear at -18° and +20° where the pattern unexpectedly plunges to nearly -28 dB, creating unintended deep notches within what should be a uniform main beam. Additionally, the baseline DNN's sidelobes are considerably worse, reaching only -17 to -25 dB in regions where -30 dB suppression is required. The error comparison reveals that the DNN–CVNN maintains low deviation throughout the main lobe (typically within 1-2 dB of target), whereas the baseline's spurious nulls represent errors exceeding 25 dB at certain angles.

Examining the excitation amplitudes and phases, the DNN–CVNN weights exhibit a coherent phase progression and smooth amplitude taper characteristic of a well-formed broadside array, effectively synthesizing the desired aperture distribution. The real-valued DNN's weights, however, show irregular phase discontinuities and amplitude fluctuations that manifest as the observed pattern distortions. This beam-shaping task highlights the fundamental advantage of complex-valued processing: the DNN–CVNN directly manipulates the phase and amplitude of array elements in a unified complex framework, enabling it to enforce the precise constructive and destructive interference required for clean pattern synthesis, while the real-valued network struggles to coordinate these coupled parameters through separate real and imaginary channels, resulting in corrupted radiation characteristics.

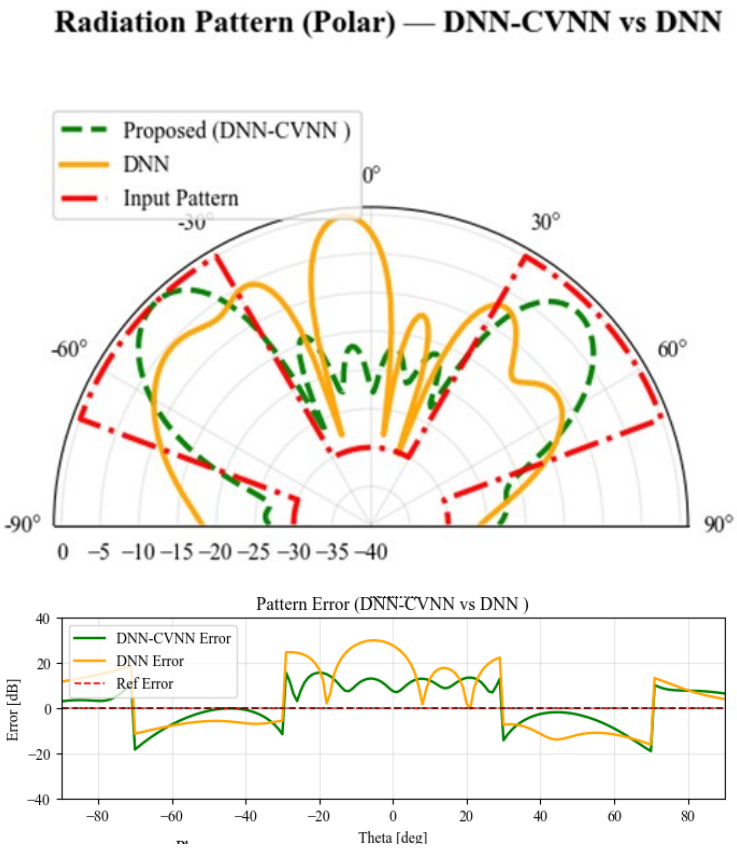

Figure 4 Radiation Pattern Synthesis: Dual-Beam Synthesis

Across all scenarios, the aggregate performance metrics favor the hybrid model. On average, the DNN–CVNN reduced sidelobe levels by several dB compared to the real-valued DNN, and it steered the main beams with sub-degree accuracy. The learning curves show that both networks eventually converge to stable solutions, but the CVNN's training is more stable and reaches a lower final error more rapidly, as expected from its physics-aware design [19]. We also note that the amplitudes predicted by the DNN–CVNN tend to follow a smooth taper (often raised-cosine or Gaussian-like), and the phases progress monotonically, making the outputs immediately usable for practical phased-array hardware. By contrast, the real-valued DNN occasionally outputs weight distributions that would require additional processing to interpret as valid antenna settings.

In this sense, the hybrid model learns "realistic" excitation vectors: when these weights are applied in CST Microwave Studio, the simulated beams match the network's predictions almost perfectly, verifying that the learned weights correspond to implementable antenna excitations (this is in line with other studies showing DL can generate valid complex excitations from desired patterns).

In summary, the proposed DNN–CVNN approach consistently outperforms the baseline real-valued DNN in our experiments. Its ability to natively handle phase information leads to better pattern conformity (main-lobe shape and direction), stronger sidelobe suppression, and more accurate multi-beam shaping across the tested cases. The CST-validated patterns demonstrate that the learned complex weights are both physically plausible and effective. These results confirm that incorporating complex-valued processing into the neural network is an effective strategy for phase-sensitive beamforming problems [20-21].

4. Conclusion

This work shows that a hybrid DNN–CVNN model can accurately learn the inverse mapping from target radiation patterns to complex excitations for an 8-element phased array at 28 GHz. By integrating complex-valued processing in the output layer, the model naturally captures amplitude–phase coupling, achieving better performance than conventional real-valued DNNs.

Across beam steering, sidelobe suppression, and broad-beam shaping, the DNN–CVNN consistently outperforms the baseline, improving sidelobe levels by 15–20 dB, maintaining sub-degree pointing accuracy, and generating smooth, physically realizable excitations. CST validation confirms that the predicted weights produce accurate far-field patterns, demonstrating practical viability for mmWave systems.

The complex-valued formulation enables direct manipulation of phase fronts and interference conditions, leading to faster convergence, more stable training, and better generalization. This makes the approach well suited for real-time adaptive beamforming in 5G/6G systems, where the trained

model generates weights in milliseconds—far faster than iterative optimization methods. The framework can be extended to larger arrays, planar architectures, and multi-band applications.

Future work includes incorporating physics-informed constraints, supporting multi-objective pattern control, quantifying prediction uncertainty, and deploying the model on edge hardware for real-time operation.

In summary, complex-valued neural networks provide an efficient and accurate solution for phased-array synthesis, bridging machine learning and electromagnetic design for next-generation wireless communication systems.

References

[1] L. Godara, "Applications of antenna arrays to mobile communications. I. Performance improvement, feasibility, and system considerations," *Proc. IEEE*, vol. 85, pp. 1031–1060, 1997.

[2] T. S. Rappaport, *Wireless Communications: Principles and Practice*, 2nd ed. Upper Saddle River, NJ, USA: Prentice Hall, 2002.

[3] S. Kumar, "6G Mobile Communication Networks: Key Services and Enabling Technologies," *J. ICT Stand.*, vol. 10, pp. 1–10, 2022.

[4] M. Dehmas, M. Challal, A. Arous and H. Haif, "A Novel Design of a Microstrip Antenna Array for Wireless Power Transfer Applications," Wireless Personal Communication, 134, pp. 581–596, March 2024.

[5] M. Li, Y. Liu, Z. Bao, L. Chen, J. Hu, and Y. J. Guo, "Efficient phase-only dual- and multi-beam pattern synthesis with accurate beam direction and power control employing partitioned iterative FFT," *IEEE Trans. Antennas Propag.*, vol. 71, pp. 3719–3724, 2023.

[6] D. R. Prado, "The generalized intersection approach for electromagnetic array antenna beam-shaping synthesis: A review," *IEEE Access*, vol. 10, pp. 87053–87068, 2022.

[7] A. Vié, "Qualities, challenges and future of genetic algorithms," *SSRN Electron. J.*, 2020.

[8] A. G. Gad, "Particle swarm optimization algorithm and its applications: A systematic review," *Arch. Comput. Methods Eng.*, vol. 29, pp. 2531–2561, 2022.

[9] M. Challal, A. Mekircha, M. D. Bendref, "Antenna Design and Optimization using AI-based Techniques," International Conference on Computational Engineering, Artificial Intelligence and Smart Systems (IC2EAIS2), 29-31 October 2025, Djanet, Algeria.

[10] L. Alzubaidi *et al.*, "Review of deep learning: Concepts, CNN architectures, challenges, applications, future directions," *J. Big Data*, vol. 8, p. 53, 2021.

[11] Y. Wang, L. Liu, and C. Wang, "Trends in using deep learning algorithms in biomedical prediction systems," *Front. Neurosci.*, vol. 17, p. 1256351, 2023.

[12] M. M. Taye, "Understanding of machine learning with deep learning: Architectures, workflow, applications and future directions," *Computers*, vol. 12, p. 91, 2023.

[13] *Recurrent Deep Learning for Beam Pattern Synthesis in Optimized Antenna Arrays*, unpublished.

[14] M. A. Abdullah *et al.*, "Antenna array pattern with sidelobe level control using deep learning," *Appl. Comput. Electromagn. Soc. J. (ACES)*, pp. 427–435, 2025.

[15] M. R. Ghaderi and N. Amiri, "Application of machine learning techniques in phased array antenna synthesis: A comprehensive mini review," *J. Commun.*, vol. 18, no. 10, pp. 629–642, 2023.

[16] M. D. Bendref, M. Challal**,** A. Mekircha, "AI-Driven Real-Time Adaptive Beam Steering for 5G Fixed Wireless Access Antenna Systems," 9th International Conference on Artificial Intelligence in Renewable Energetic Systems (ICAIRES), 28-30 October 2025, Mostaganem, Algeria.

[17] Z. A. I. B. Alam *et al.*, "AESA antennas using machine learning with reduced dataset," *Radioengineering*, vol. 33, no. 3, p. 397, 2024.

[18] A. B. Suksmono and A. Hirose, "Performance of adaptive beamforming by using complex-valued neural network," in *Proc. Int. Conf. Knowledge-Based Intell. Inf. Eng. Syst.*, Berlin, Germany: Springer, 2003.

[19] R. Abdalla, "Complex-valued neural networks—Theory and analysis," *arXiv preprint* arXiv:2312.06087, 2023.

[20] S. Oh, S. Pyo, and H. Jang, "PhaseNet: A deep learning framework for reflectarray antenna gain prediction by integrating 2D phase maps and angular embeddings," *Mathematics*, vol. 13, no. 21, p. 3509, 2025.

[21] J. Bassey, L. Qian, and X. Li, "A survey of complex-valued neural networks," *arXiv preprint* arXiv:2101.12249, 2021.